Further Improvement of VAST for Analysis and Design of Composite Propellers

Report for: W7707-186266/001/HAL

Name of client: Transport Canada

Report no.: TR-22-46

Project no.: 21.28050

Revision no.: 01

19 March 2024

Summary

Further Improvement of VAST for Analysis and Design of Composite Propellers

Project Number: 21.28050

Authors: L. Jiang

Security classification of this Report: Distribute only after client's acceptance

Report no.:	Revision no.:	Report date:
TR-22-46	01	19 March 2024

Prepared by:	Reviewed by:	Approved by:
Lei Jiang Lead Specialist	Tamunoiyala Koko Team Leader, Risk and Reliability	Dave Whitehouse Technical Manager

Registered name:	Martec Limited
Correspondence address:	Lloyd’s Register Applied Technology Group 237 Brownlow Ave, Suite 200 Dartmouth, NS B3B 2C7
Contact:	Lei Jiang T: 1 (902) 417 2482 E: Lei.Jiang@lr.org

Martec Limited is a member of the Lloyd’s Register Group, doing business as the Applied Technology Group

Client name and address:
Transport Canada
330 Sparks Street, Place de Ville,
Tower C, 18th Floor (AHSB), Ottawa
ON K1A 0N5

Client contact:
Matthew Cooke
T: +1 343-543-3497
E: matthew.cooke@tc.gc.ca

Document control

Revision history

Revision No.	Date	Revision
00	22 November 2022	
01	19 March 2024	Implemented Tsai-Wu failure criterion

Proprietary Notice

Executive summary

This report describes work performed towards the Work Package 2-1 (WP2-1) in a project concerning design of composite propellers for noise reduction [1]. This work package involves refinement and further development of the VAST finite element program for use in the Trident/PVAST system and the associated MARIN and CRS software tools for improved analysis and design of composite propellers. Three objectives were accomplished in this work:

First, the quadratic shell element in VAST was further enhanced to make it suitable for incorporation into the ComPropApp system. These enhancements included extension of the load modelling capability for consistency with the 20-noded solid element previously incorporated in ComPropApp. Also implemented in the shell element was the capability for outputting the results in the Tecplot format. These Tecplot files were generated based on the 16-noded option of the shell element so the complex geometry of the propellers can be accurately modelled and displayed. This shell element had been extensively tested for composite propeller analyses through collaboration with MARIN.

Second, the previously observed stress-softening behaviour in VAST nonlinear steady-state solutions for propellers was extensively investigated. After checking the nonlinear finite element formulation and its implementation in VAST, various details of the finite element propeller models were examined. This examination led to the discovery that the atmospheric pressure was included in the external load distribution. Inspired by this finding, a simple test case involving a cantilever beam was created and analysed using both VAST and LS-DYNA. This numerical exercise confirmed that the unrealistic stress-softening characteristics shown in the VAST solution was caused by the application of the atmospheric pressure that resulted in compression in the thickness direction. It has been indicated that if the atmospheric pressure is eliminated from the external load, VAST and LS-DYNA produced identical nonlinear solutions. For this reason, the temporary piecewise linear algorithm implemented in the earlier VAST was no longer required, so it was removed in the current version of the VAST solver.

Third, the Tsai-Wu failure criterion was successfully extended to nonlinear static analysis of composite structures and tested using the ORCA composite propeller model.

Contents

List of Figures

List of Tables

1. Introduction

This report describes work performed towards the Work Package 2-1 (WP2-1) in the Transport Canada (TC) funded project concerning the design of composite propellers for noise reduction [1]. This work package involves refinement and further development of the Trident/PVAST system and the associated MARIN and CRS software tools for improved analysis and design of composite propellers.

The following requirements are addressed in this report:

1. The Trident/PVAST application within the ComPropApp tool needs to be enhanced with the provision of composite shell elements to provide greater flexibility in propeller modelling. Currently, only the option to model the propeller with multi-layered composite solid elements is available. This limits the useability of the App, as some composite propeller designers base their analysis on shell elements. Having the shell element capability in ComPropApp will more easily enable comparison of the ComPropApp tool to other studies, as a means of further validating/ verifying the ComPropApp tool's capabilities.

2. Improvements also need~~s~~ to be made to the finite element solution engine VAST [2] for more accurate simulations of nonlinear steady state applications. Currently, an ad hoc multi-linear solution algorithm was utilized in the Trident/PVAST suit for modelling the flexible propeller behaviour. A more robust nonlinear solution algorithm will be implemented in this task.

In addition to the above requirements, the Tsai-Wu failure criterion, which was originally implemented for linear analysis, will be extended to nonlinear static analysis to detect the failure of composite propellers during large deformations.

The VAST-related modifications, investigations and verifications are documented in the following sections of this report.

2. Provision of Shell Element for ComPropApp

2.1 Modification of the Shell Element

The 8-noded shell element is the very first element implemented in the VAST finite element program [2] and had been extensively verified and validated over the past years. One of the unique features of this element is it permits the user to define the element geometry using the 16 geometric nodes located on the top and bottom surfaces, respectively as indicated in Figure 2-1(a). However, the actual finite element calculations are still carried out in terms of the displacement nodes in the mid-surface as indicated in Figure 2-1(b). The conversion from the 16-noded to 8-node element formulations is performed automatically inside the VAST solver by enforcing the standard kinetic constraints to the displacement field. This unique implementation provided the advantage of high accuracy modelling of complex problem geometry, such as propellers and in the meantime, maintained the convenience of the shell element formulation.

In the present work, this element type was further improved to meet all the requirements of ComPropApp for steady-state and dynamic analyses of isotropic and composite propellors. This further development included modification of the LOAD module to achieve complete consistency between the shell and solid elements, and implementation of the Tecplot file format into the shell element subroutines to output results in the Tecplot format for all analysis options required by ComPropApp.

2.2 Verification of the Shell Element

To verify the shell element for propeller analyses, the standard test cases were considered, which involved nonlinear steady-state, modal and linear unsteady analyses of both isotropic and composite propellers. In addition to the binary results files, the following Tecplot files were also generated by VAST from these analyses. All these Tecplot files are based on the 16-noded element definition described above, so the propeller geometry can be realistically displayed in the Tecplot imagines, just like those from the solid elements.

Table 2-1: Tecplot files generated by VAST for different analysis options

File Extension	Description	Analysis Option
tcp	Coordinates, displacements, nodal stresses	Steady, Unsteady
tdm	Coordinates, mode shapes	Modal
tsf	Coordinates, element connectivity, safety factor	Unsteady, composite

Using these results files, Tecplot imagines were created successfully by MARIN [3] for the displacement contours, dry modeshapes, element stresses and safety factors, as depicted in Figure 2-2 to Figure 2-5.

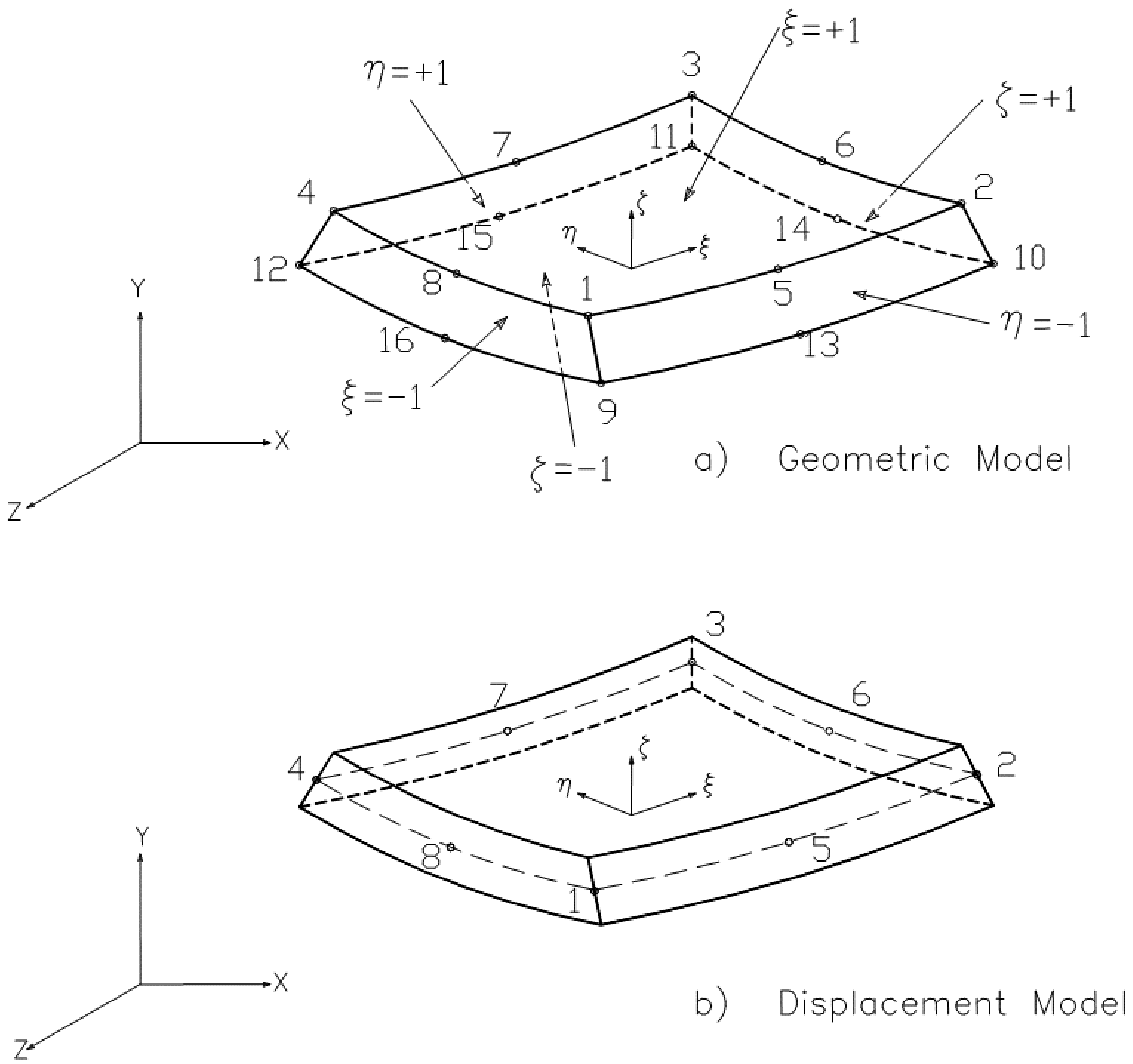

Figure 2-1: Geometric and displacement models of the quadratic shell element in VAST

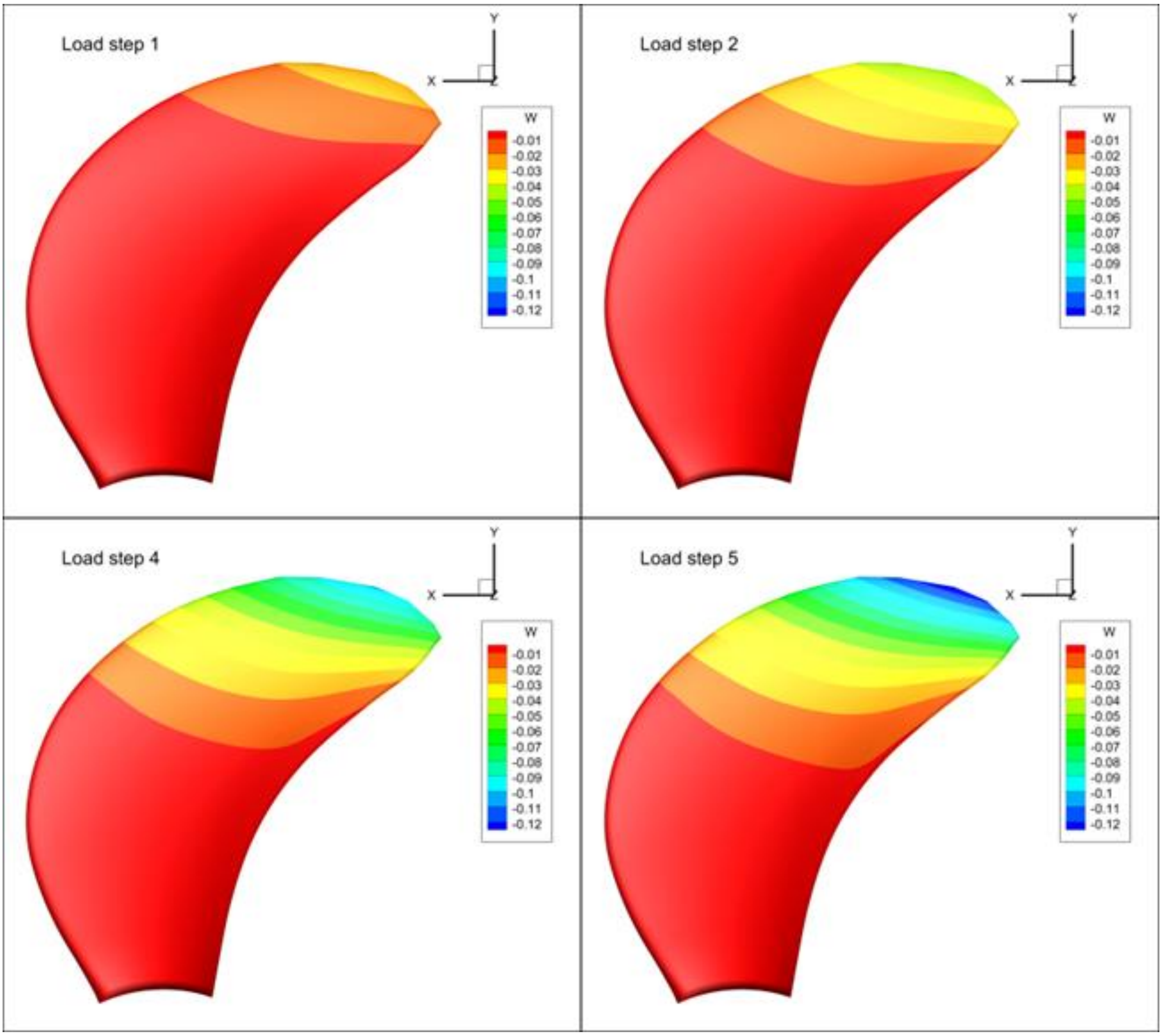

Figure 2-2: Typical Tecplot imagines of displacement contours from nonlinear steady state analysis.

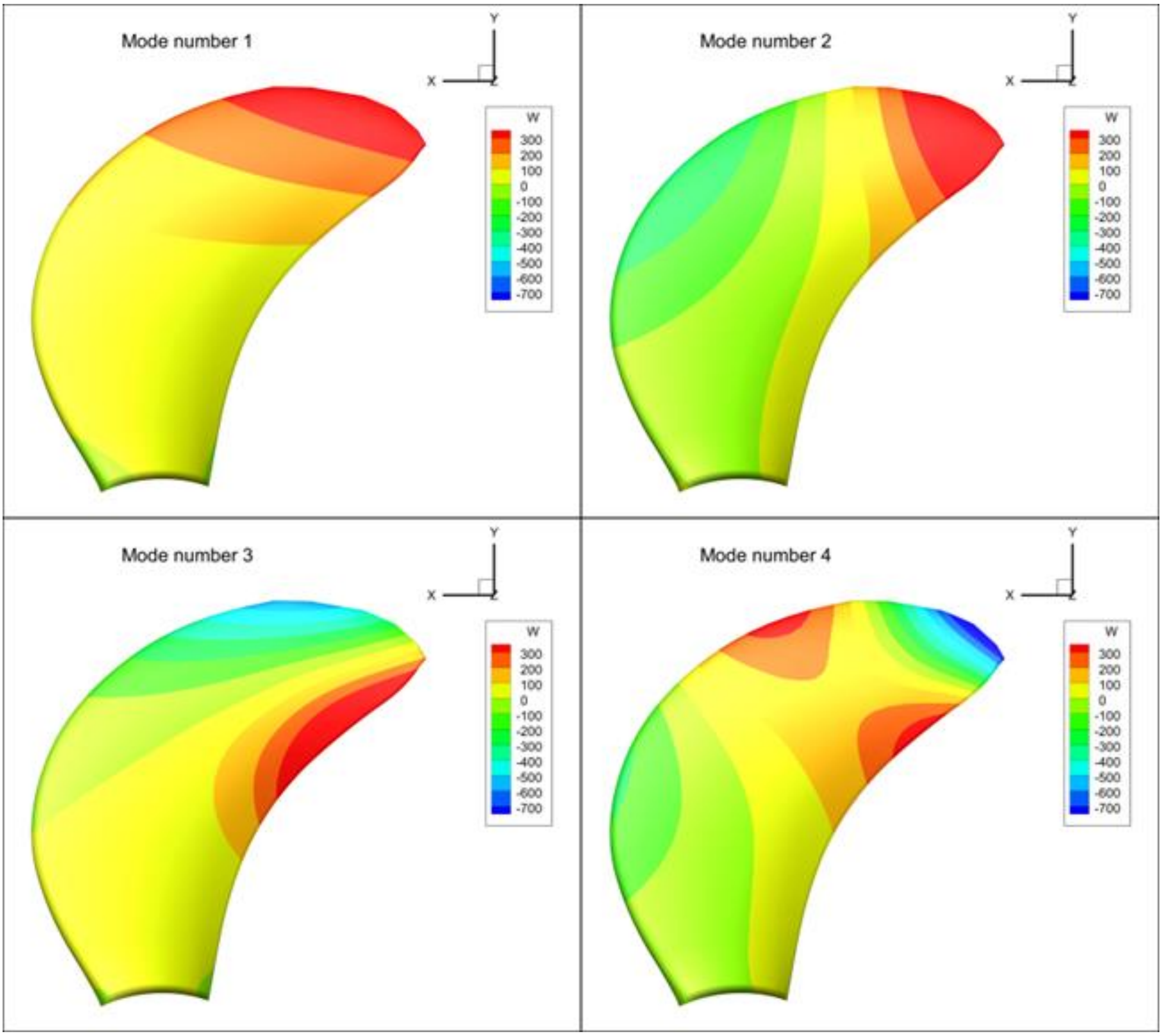

Figure 2-3: Typical Tecplot imagines of mode shapes from modal analysis.

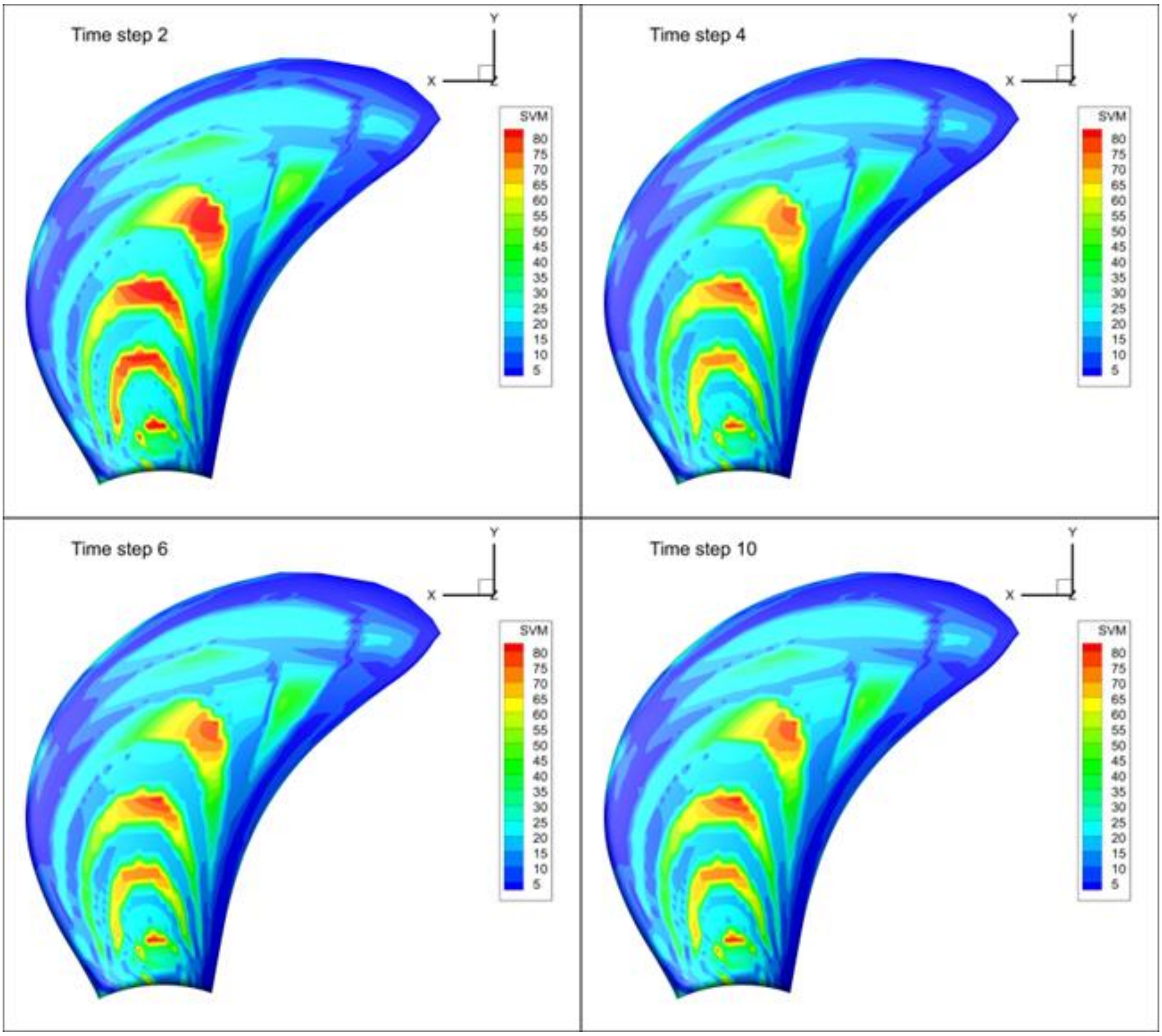

Figure 2-4: Typical Tecplot imagines of von Mises stresses from linear unsteady analysis.

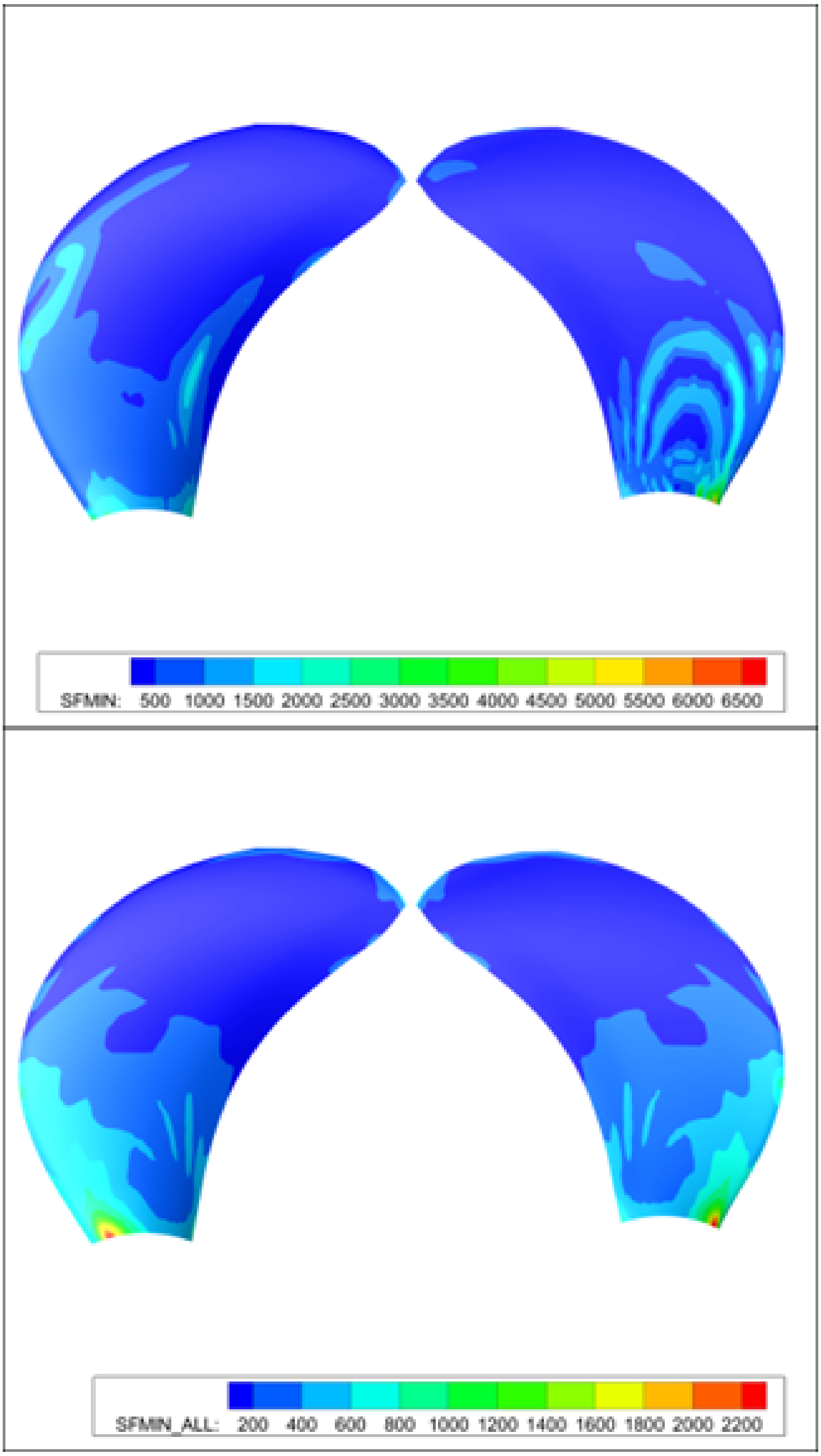

Figure 2-5: Typical Tecplot imagines of safety factors for failure check of composite propellers.

3. Investigation of Solid Element for Nonlinear Static Analysis of Propellers

3.1 The Unrealistic Stress Softening Behaviour

Earlier numerical analyses confirmed that the 20-noded solid element provided in VAST can accurately predict displacements and stresses of isotropic and composite propellers in linear static and dynamic analyses. These capabilities were verified using a C4-40 propeller model made of SikaBlock (Young's modulus = 800 MPa, Poisson's ratio = 0.3, mass density = 650 kg/m3) at a ship speed of 1.02 m/s and rotation rate of 5 rev/s. However, for nonlinear steady state problems, the VAST solid element produced overly soft nonlinear responses as indicated in Figure 3-1. This stress-softening behaviour was found to be inconsistent with both the experimental results and the predictions of other finite element programs, such as LS-DYNA [4].

Because the expected response of the propeller is nearly linear within the loading range of interest, a piecewise linear solution algorithm was temporarily provided in VAST to ensure continuation of ComPropApp development and testing. In the meantime, a careful investigation was conducted to gain more insight of the problem and find out a remedy for it. This investigation is described in the present section.

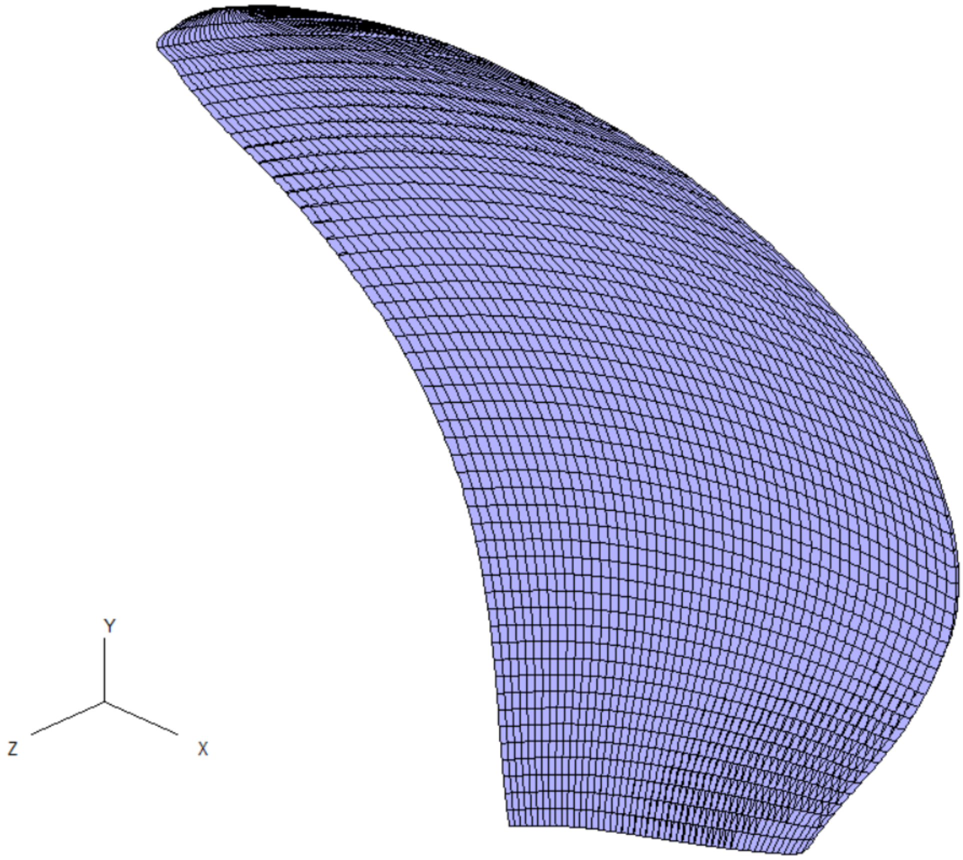

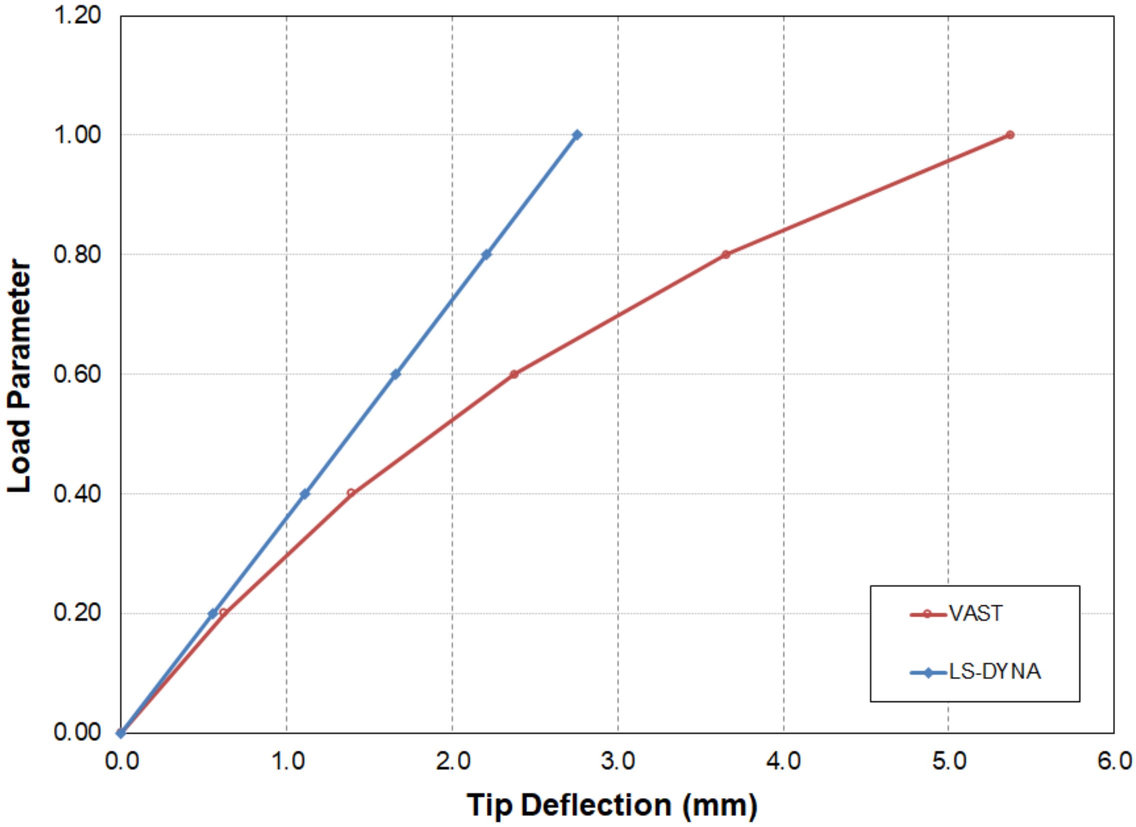

Figure 3-1: Solid element propeller model of the standard test case and the load-tip deflection curves predicted by VAST and LS-DYNA.

3.2 Further Verification of the Solid Element Formulation

The geometric nonlinear capability of the 20-noded solid element in VAST was implemented based on the Total Lagrange Formulation. This is a highly mutual finite element formulation and has been documented in numerous scientific publications and textbooks, such as [5]. In the present work, the nonlinear element formulation of the solid element and its implementation in VAST, especially the source code for calculating the Green-Lagrange strain tensors and the geometric stiffness matrix, were carefully checked. Unfortunately, no error was found.

Extensive numerical tests were then performed using highly nonlinear test cases to check the reliability of the VAST solid element. Among these test cases are the clamped-clamped circular arch, the hinged spherical shell, and the simply supported cylindrical shell. The original and deformed solid element meshes and the predicted load-deflection curves for these test problems are presented in Figure 3-2 and Figure 3-4. Because the shell element in VAST was already verified against the published solutions, the shell element solutions were utilized to verify the present solid element results. The good agreement between the load-deflection curves produced by the shell and solid elements for all these nonlinear test cases confirmed the accuracy of the solid element in VAST for analysis involving strong geometric nonlinearities.

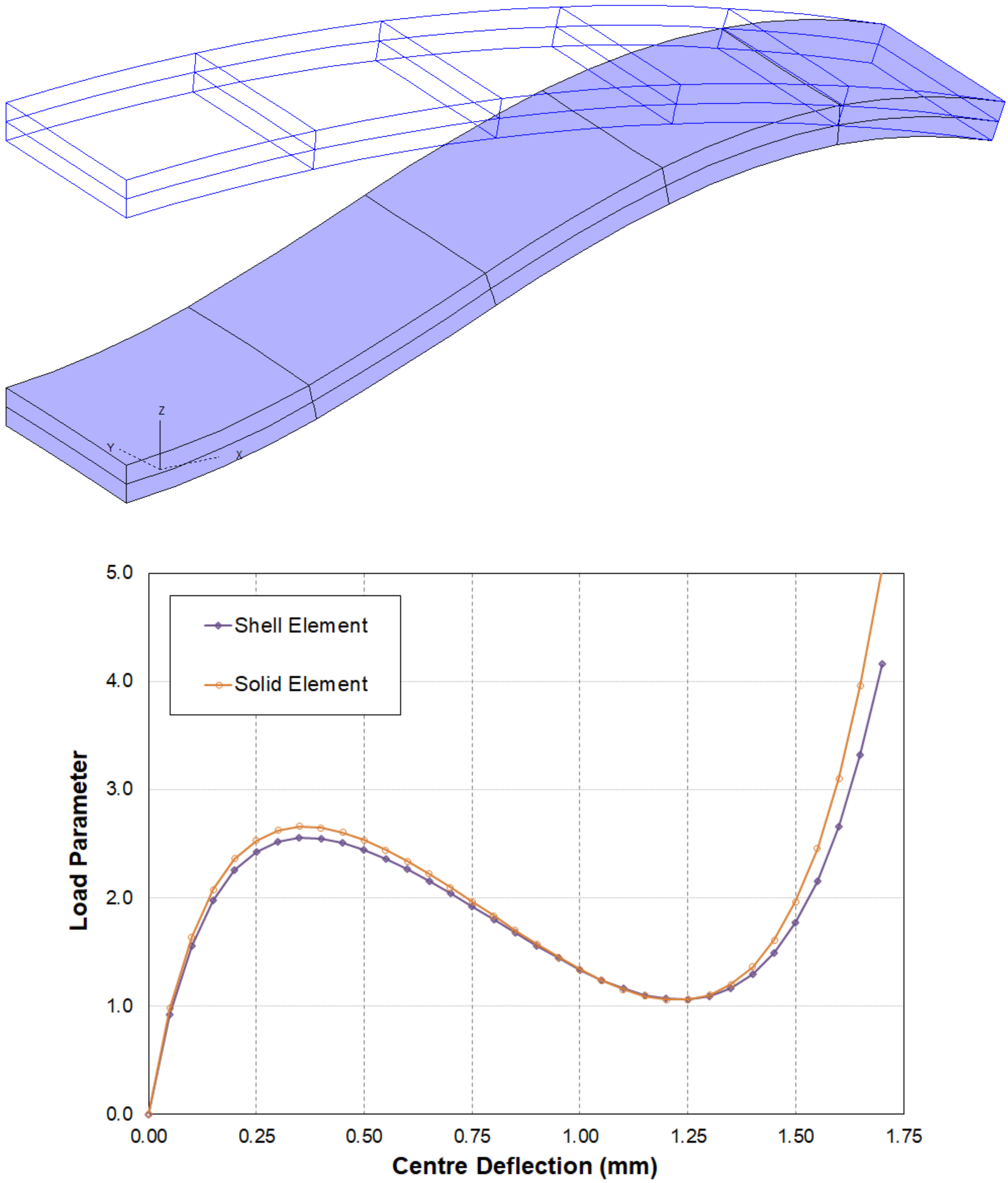

Figure 3-2: Original and deformed solid element model of a circular arch and the load-deflection curves predicted by VAST using shell and solid elements.

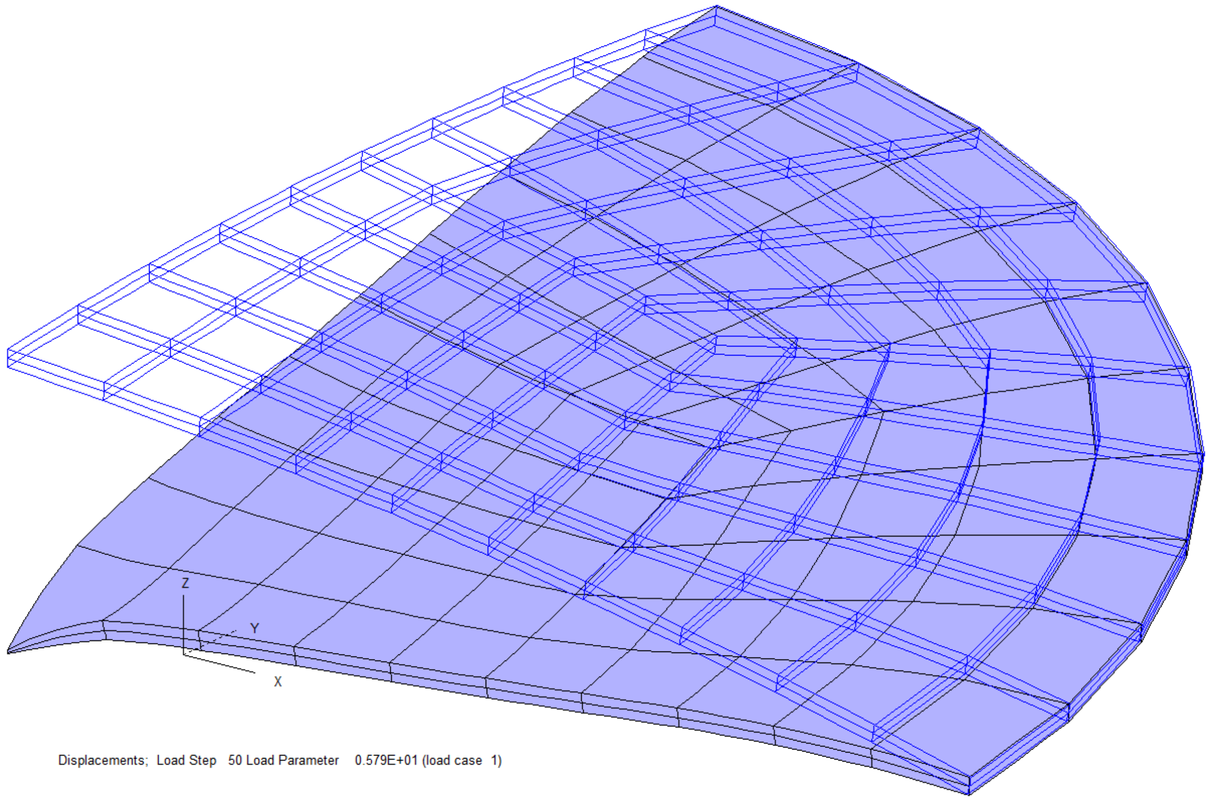

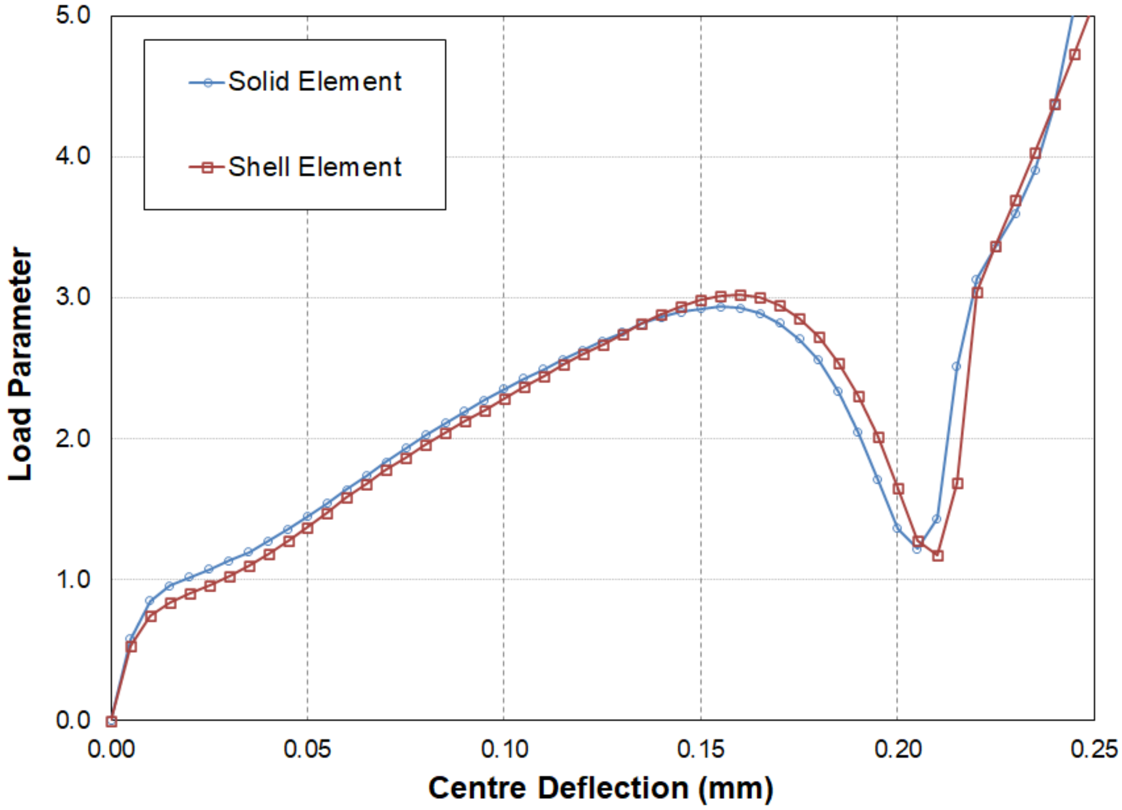

Figure 3-3: Original and deformed solid element model of a spherical cap and the load-deflection curves predicted by VAST using shell and solid elements.

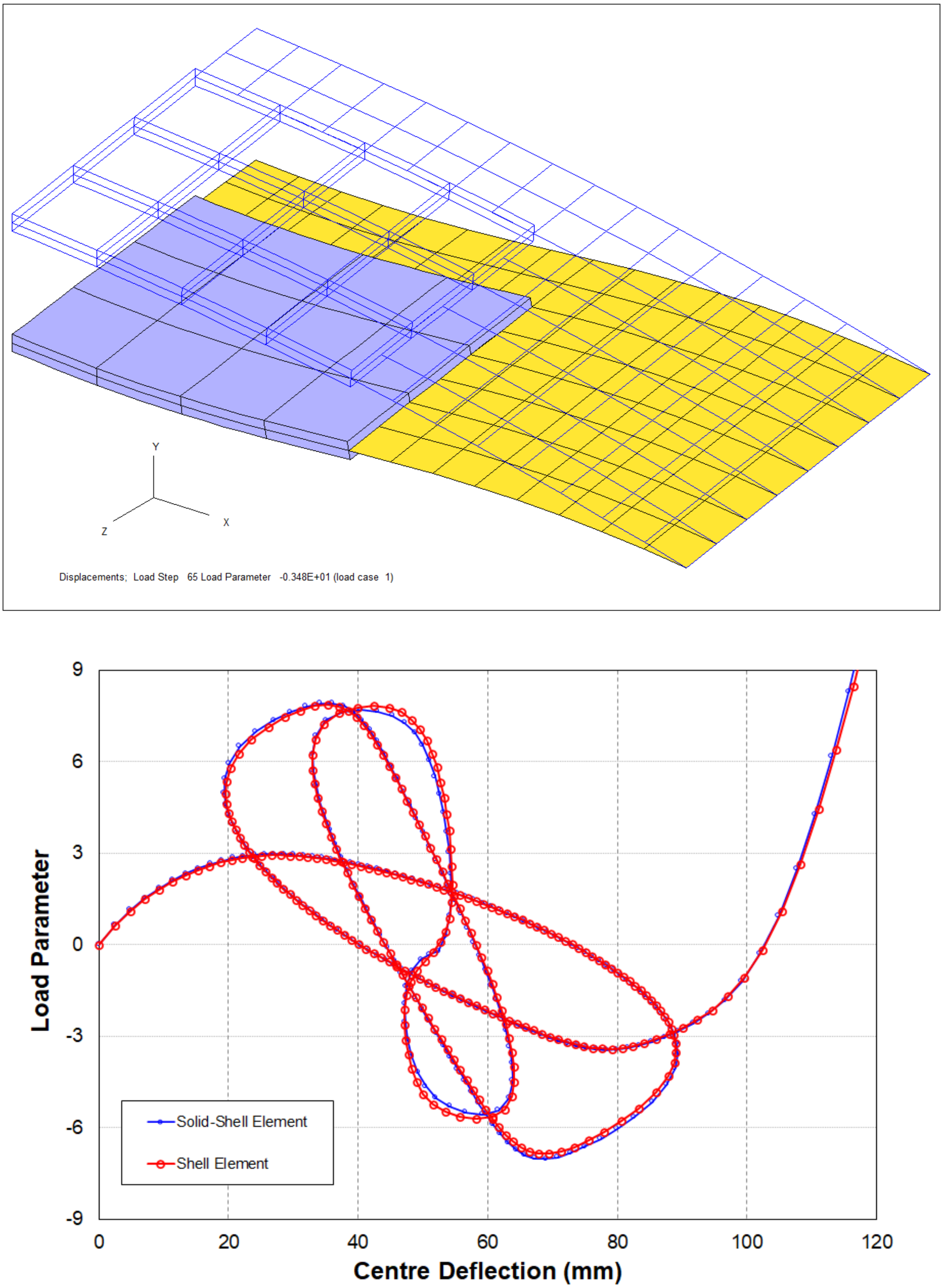

Figure 3-4: Original and deformed solid-shell element model of a cylindrical shell and the load-deflection curves predicted by VAST using shell and solid elements.

3.3 Identification of the Source of the Problem

Due to the inability of identifying problems in the finite element formulation and the VAST program, we turned our attention on the definition of the propeller model. Examination of a typical propeller model indicated that the propellor was loaded on both faces (Face 1 and Face 2 as indicated in Figure 3-5) by positive pressures which point towards the interior of the propellor.

Because these pressures are of similar magnitudes as indicated in Figure 3-5, they would only generate small net forces for bending deformations of the blade, but significant compressive stresses in the thickness direction. It was suspected that these compressive stresses caused a reduction of the tangent stiffness and led to a stress-softening behaviour.

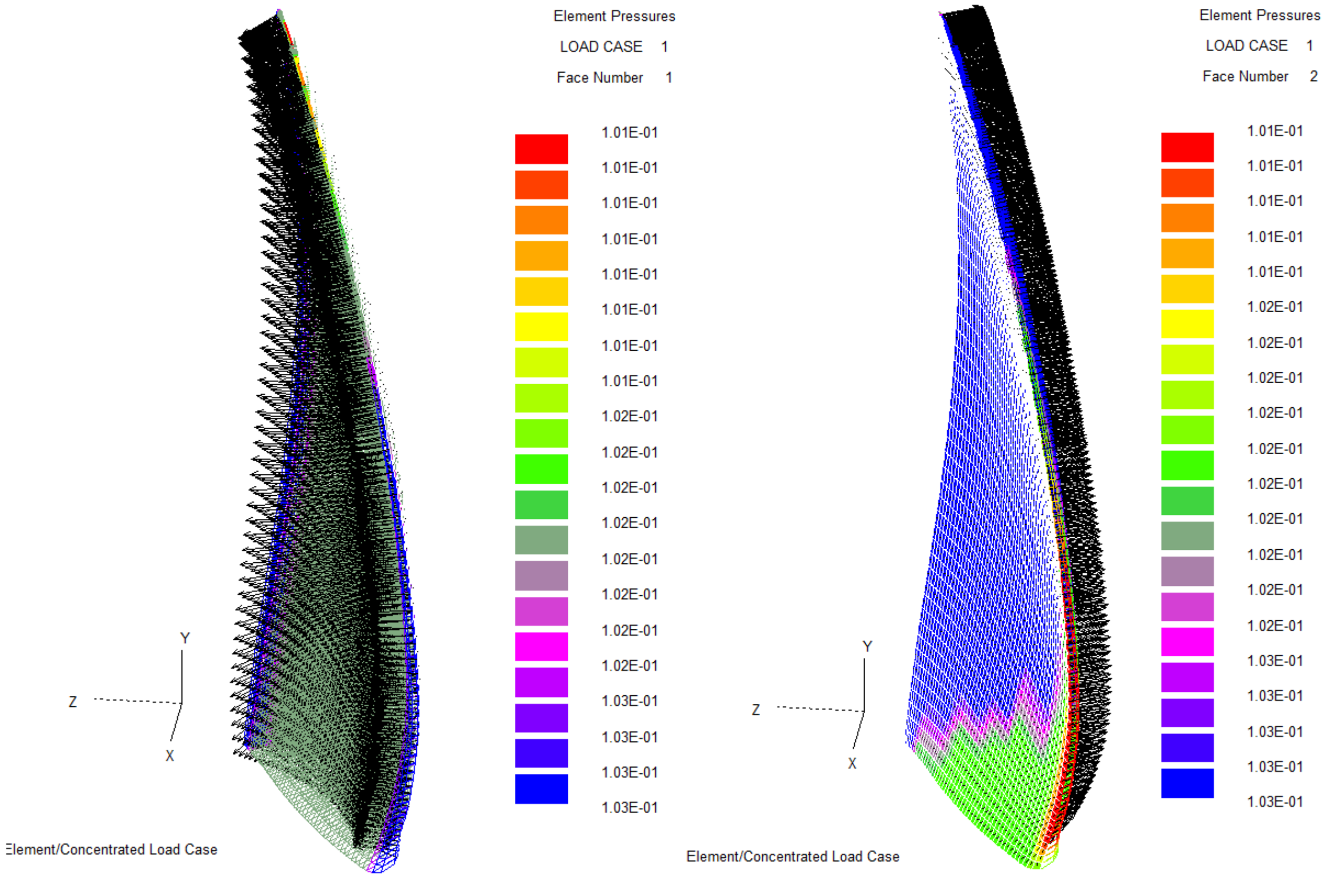

Figure 3-5: Typical pressure distributions on the back and front faces of a propeller model for steady state analysis in ComPropApp.

The findings described above inspired development of a simple test model involving a cantilever beam indicated in **Figure 3-6.** The dimensions of the beam were 5.0m x 1.0m x 0.2m and the typical material properties of steel were applied, including Young's modulus of 207000 MPa and Poisson's ratio of 0.3. This beam was loaded by a positive pressure (pointing into the interior) of 2.5 MPa on its top surface, but a negative pressure (pointing away from the interior) of 2.5 MPa on its bottom, so a net distributed load of *p*=5.0 MPa was applied. To verify the geometrically nonlinear results produced by the 20-noded solid element in VAST, the same test case was also solved by using the 8-noded and 4-noded shell elements in VAST. The original and deformed meshes of the 20-noded solid element and load-deflection curves predicted by all three elements are presented in **Figure 3-7**. An excellent agreement between all solutions was obtained.

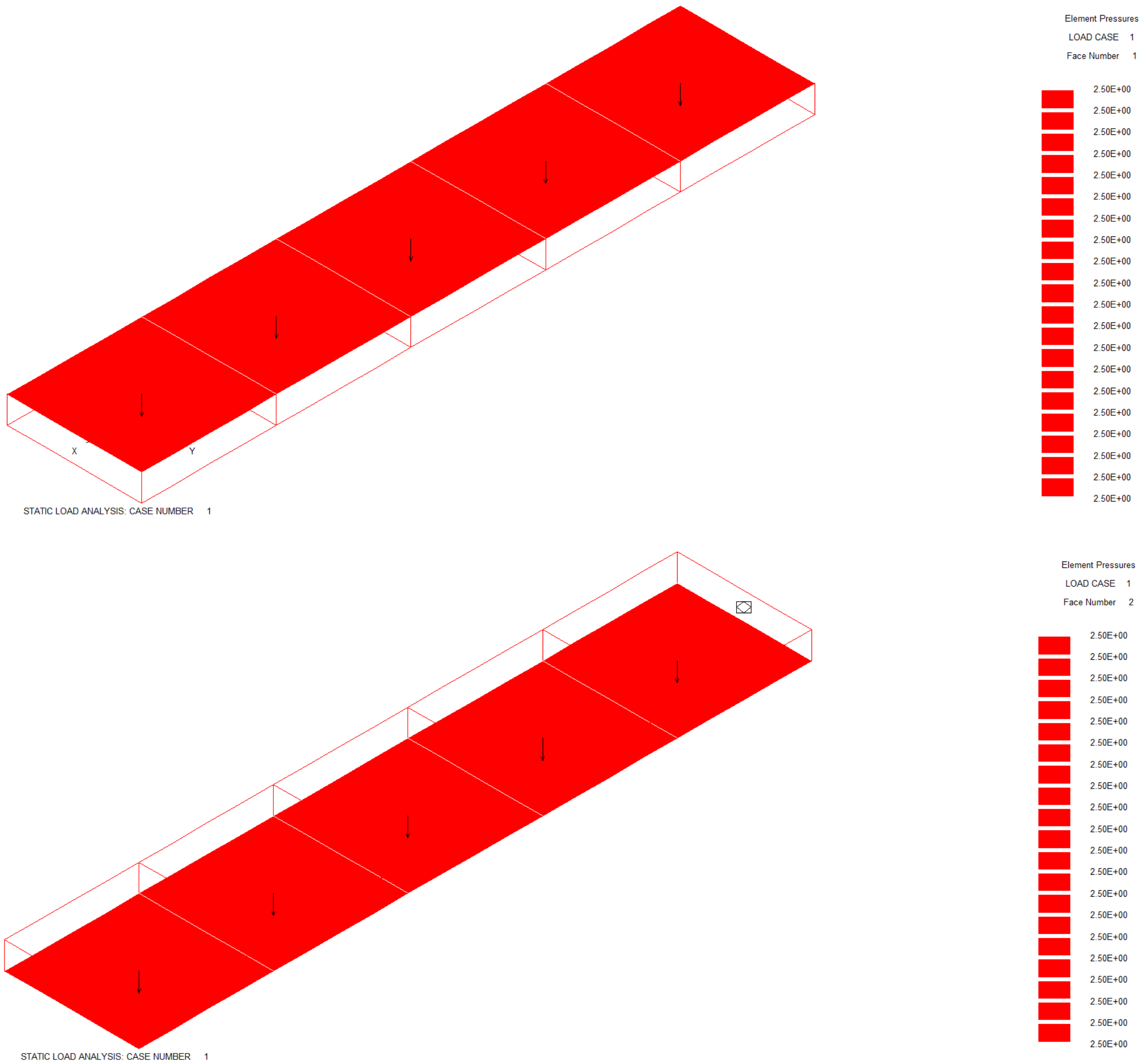

Figure 3-6: Pressures applied to solid-shell element model of the cantilever beam to generate bending deformations.

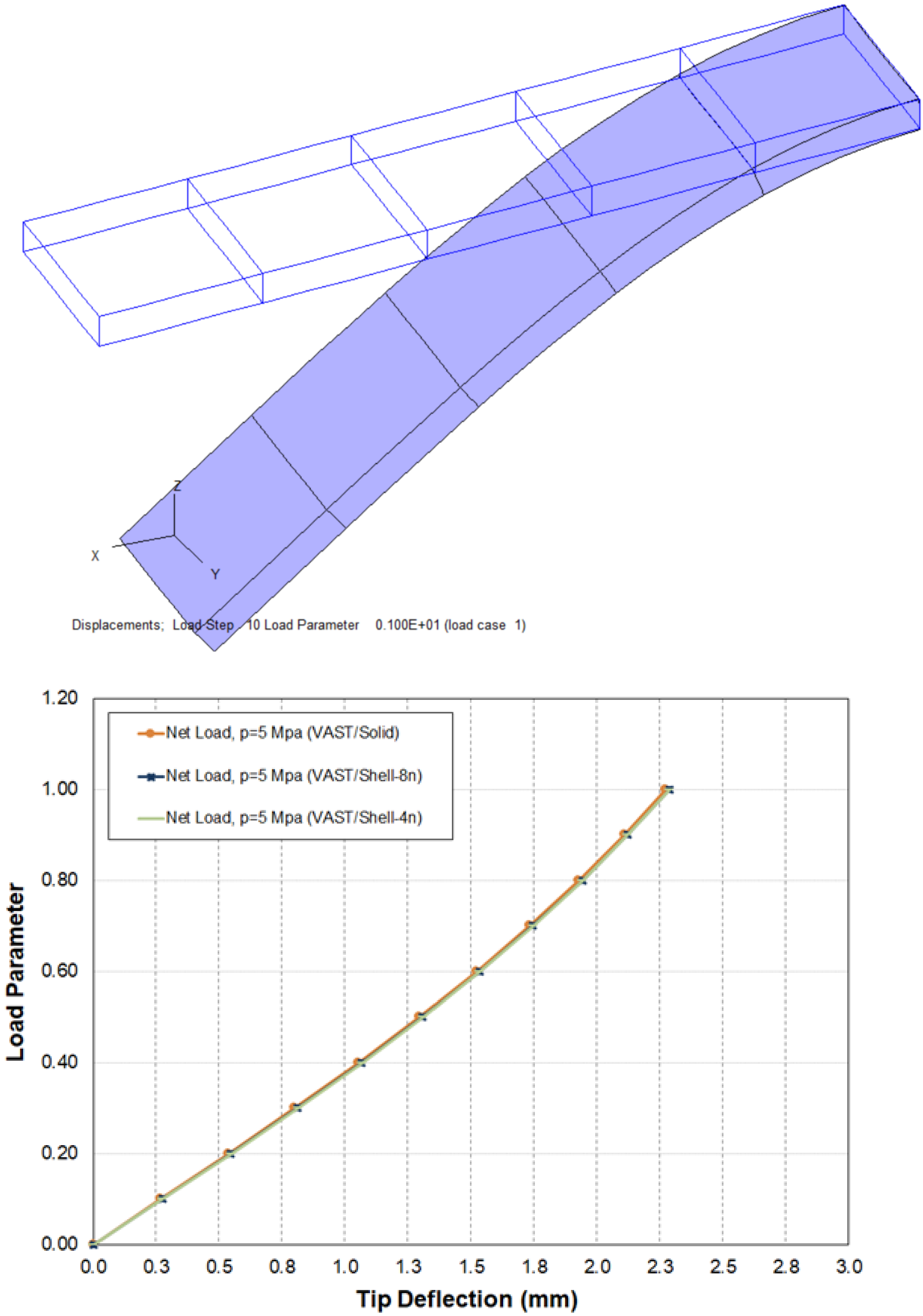

Figure 3-7: Original and deformed solid element model of a cantilever beam and the load-deflection curves predicted by VAST using shell and solid elements.

In the subsequent load cases, a set of positive pressures of equal magnitude, *P*, acting on both the top and bottom surfaces as indicated in Figure 3-8, was added to the net load of *p*=5.0 MPa described before. It should be noted that although these additional pressures are self-equilibrium and do not contribute to the net forces, they do produce compressive stresses in the thickness direction of the beam. By reversing the sign of *P*, tensile stresses can also be generated in the thickness direction.

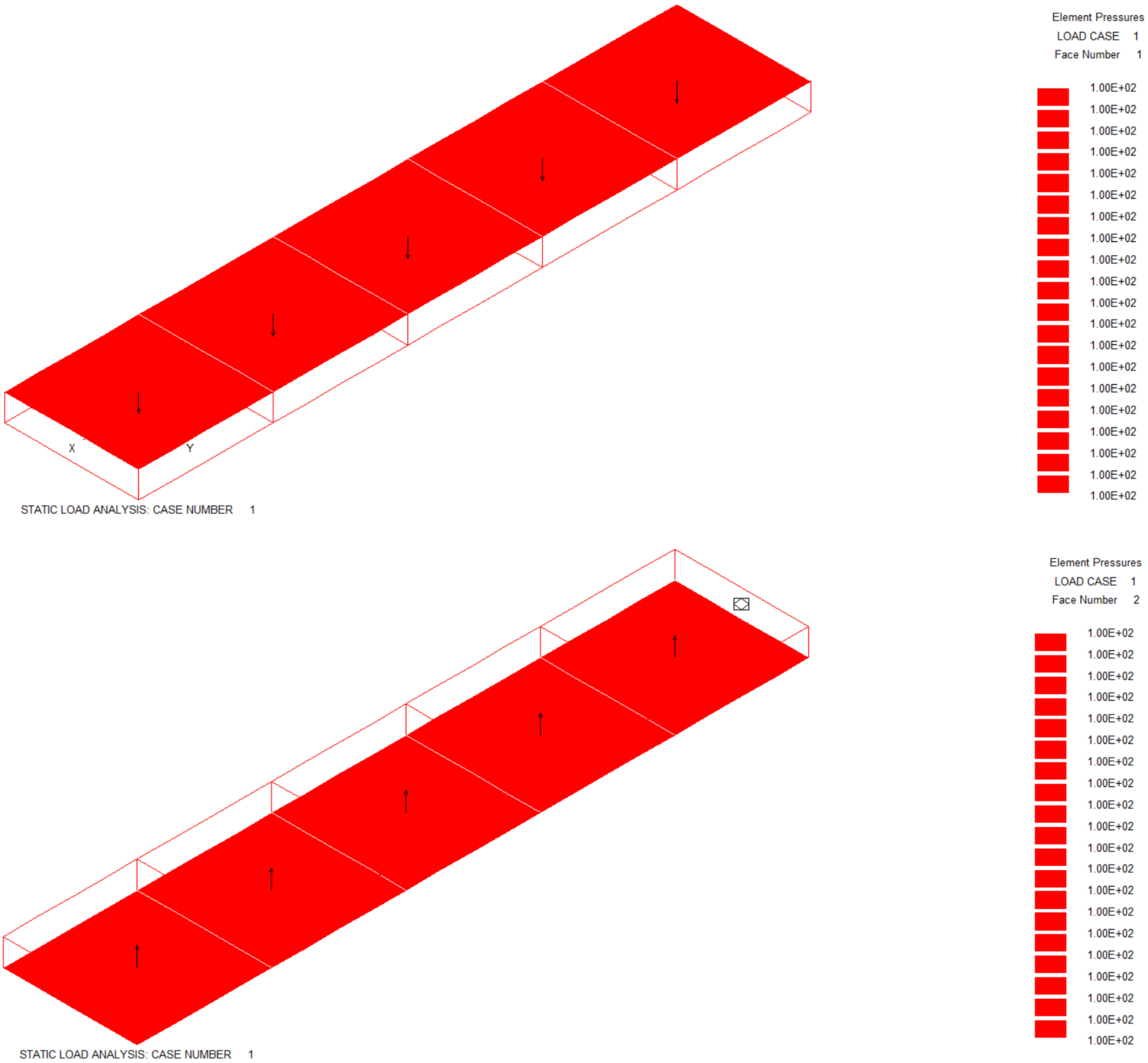

Figure 3-8: Additional pressures applied to solid-shell element model of the cantilever beam to generate compressions in the thickness direction.

The influence of the additional pressures, P, on the VAST-predicted nonlinear behaviour was presented in **Figure 3-9**. These results confirmed that the stresses in the thickness direction do have a significant impact on the nonlinear solutions of the 20-noded solid element where compressive (tensile) stresses through the thickness would lead to stress-softening (hardening) responses, respectively.

Although this trend seemed to be reasonable and was in qualitative agreement with the basic concept of solid mechanics, its magnitude was significantly greater than expected. Because the influence of these additional pressures could not be captured by the shell element (due to the basic kinetic assumption in the shell theory), the 20-noded solid element in LS-DYNA [4] was utilized to provide reference solutions for comparison. The load-deflections curves obtained from VAST and LS-DYNA for various P values are presented in **Figure 3-10**. These results indicated that when *P*=0, VAST and LS-DYNA solutions are in close agreement. For load cases involving non-zero *P*, LS-DYNA predicted the same trend as VAST, but a significantly less influence.

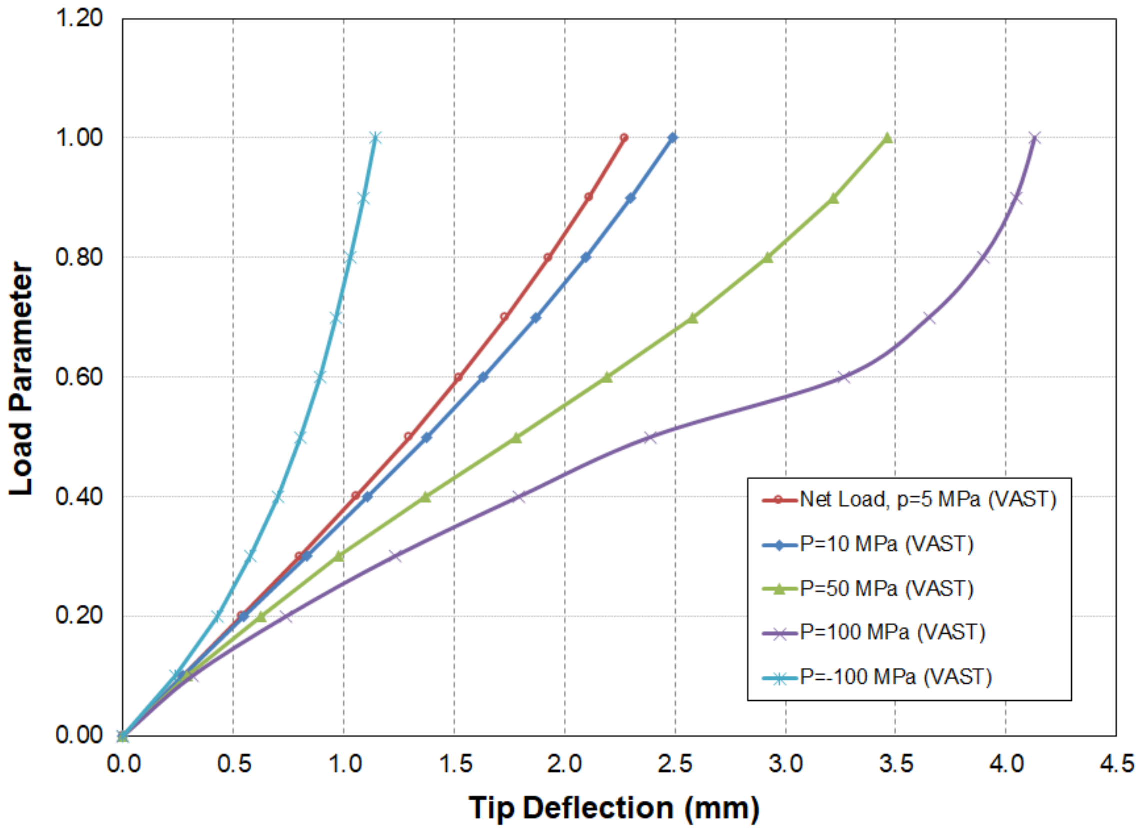

Figure 3-9: Load-deflection curves predicted by solid element in VAST for different magnitudes of the additional pressure loads.

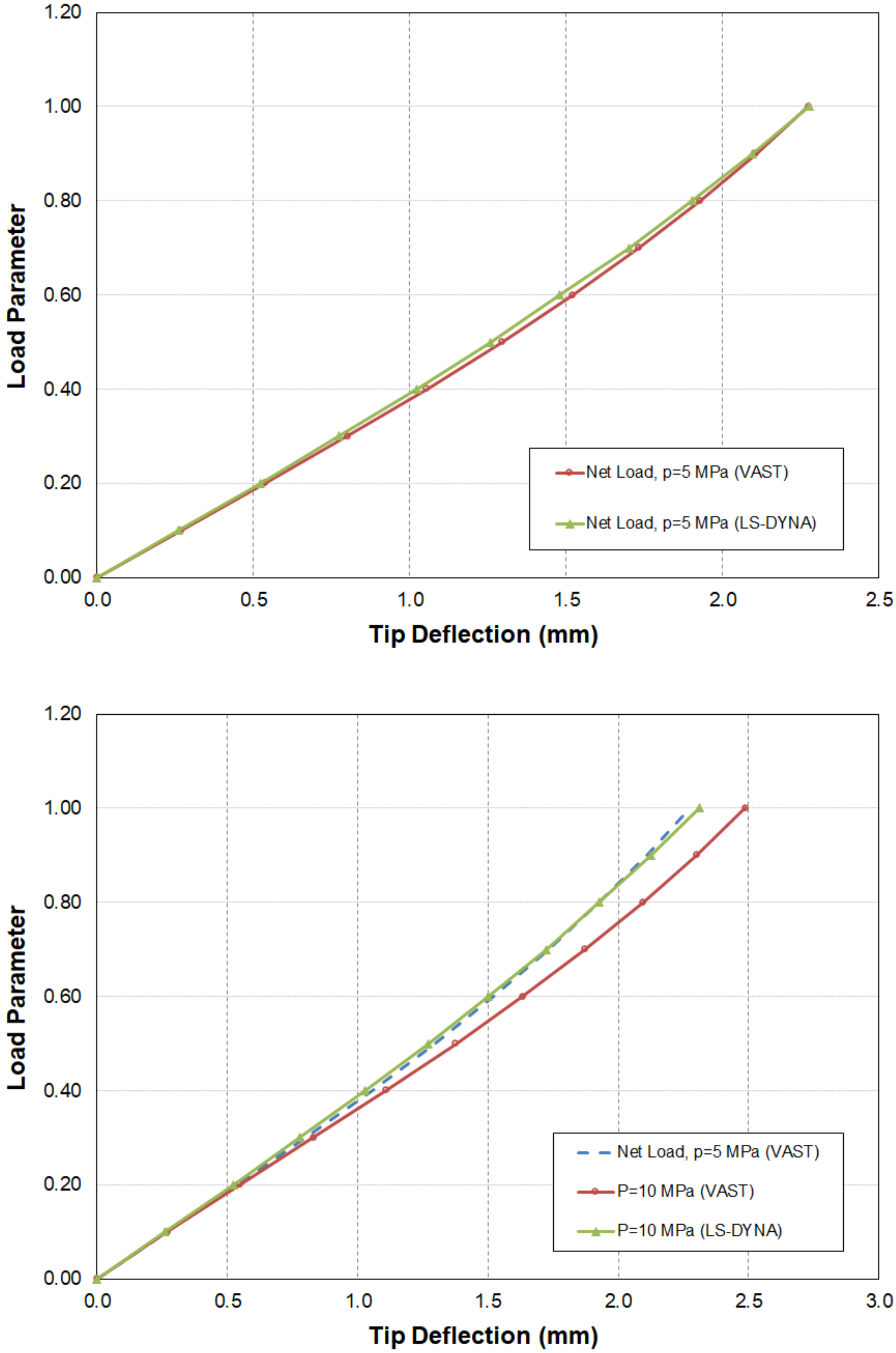

Figure 3-10: Comparison of VAST and LS-DYNA predicted load-deflection curves using solid elements for different magnitudes of the additional pressure loads.

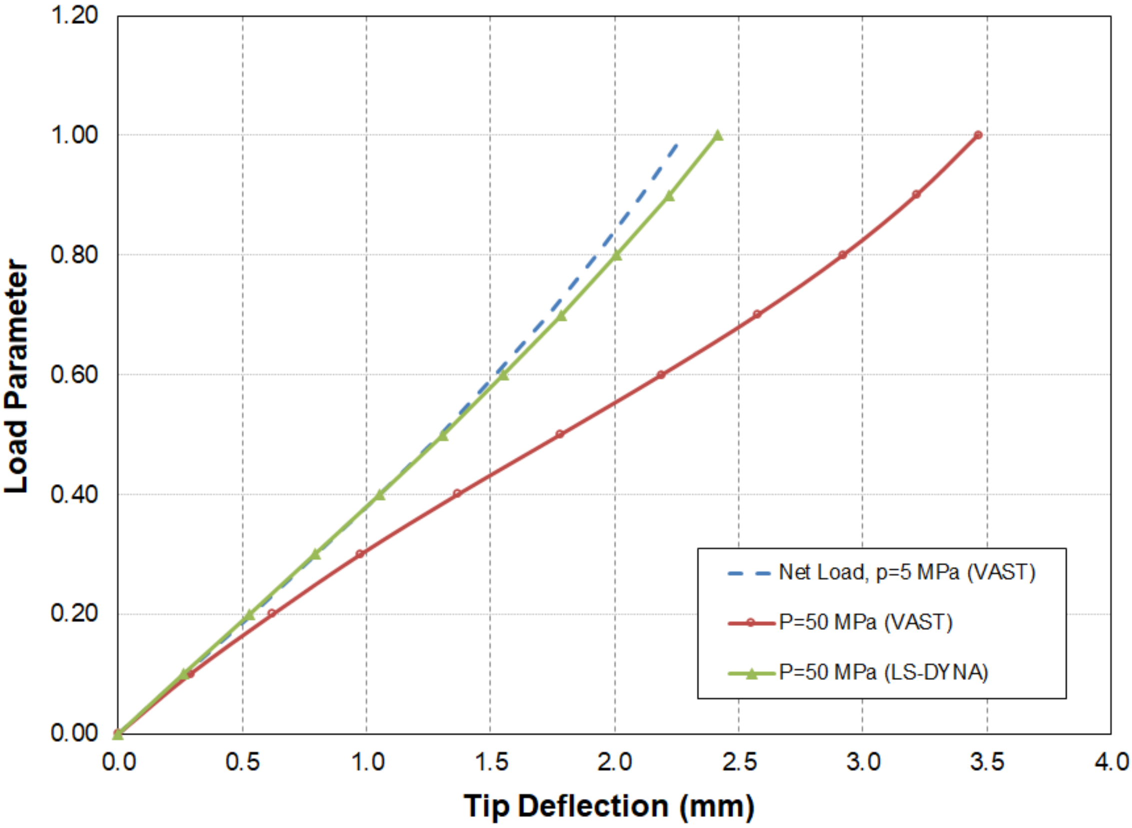

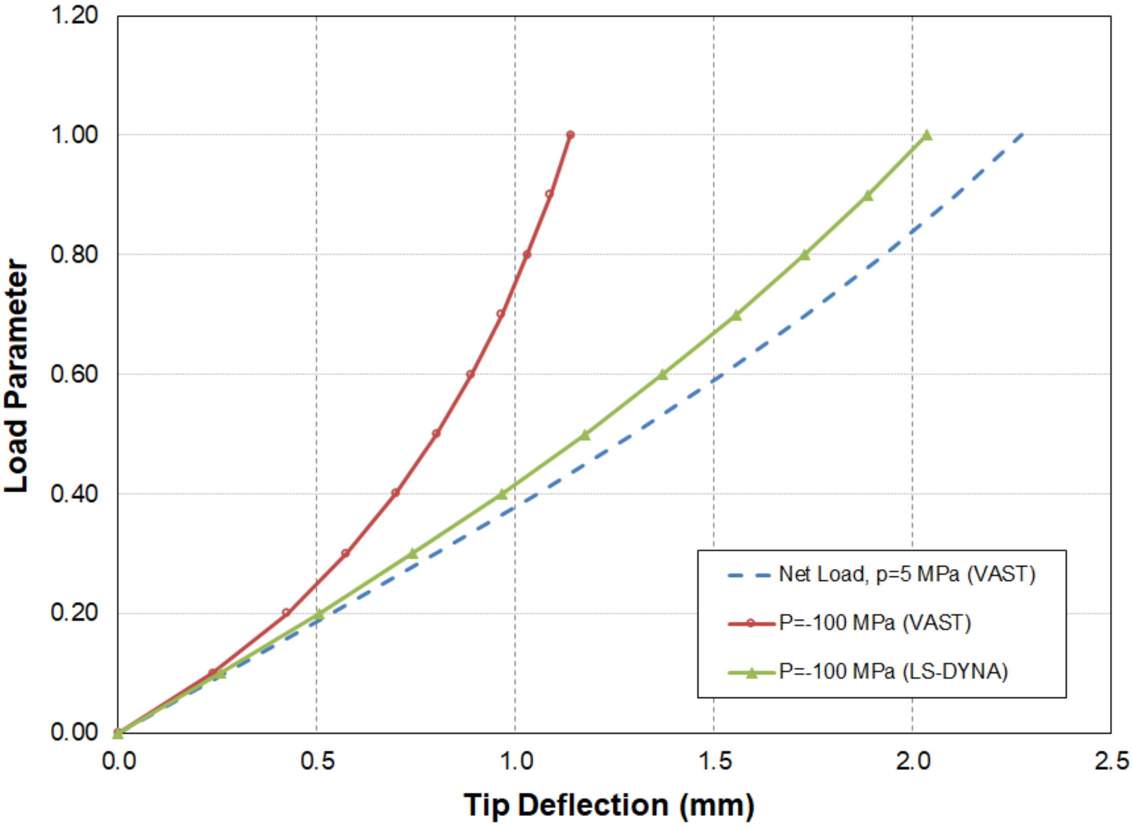

Figure 3-10 (Continued): Comparison of VAST and LS-DYNA predicted load-deflection curves using solid elements for different magnitudes of the additional pressure loads.

3.4 Proposed Solution

Although the present investigation did not lead to the discovery of any errors in the nonlinear finite element formulation and its implementation in VAST, it did reveal the root cause of the stress-softening behaviour, so a remedy to the problem could be developed.

An examination of the load definition in the propeller model indicated that the rather unique pressure distribution depicted in Figure 3-5 was due to the inclusion of the atmospheric pressure, P_{int}. Because the atmospheric pressure is normally ignored in structural analysis in air, it becomes arguable whether it should be removed from the external load for propeller analysis as well.

To quantify the influence of the atmospheric pressure on the predicted nonlinear response, VAST and LS-DYNA analyses were repeated using pressure distributions corresponding to the peak speed of the propeller, but with and without the atmospheric pressure. These load cases are indicated as *Pint* and *NoPint*, respectively. The VAST and LS-DYNA solutions are compared in Figure 3-11. These results indicated that when the atmospheric pressure was included (*Pint*), VAST produced a much softer response than LS-DYNA, like those shown in Figure 3-1. However, when the atmospheric pressure was removed from the pressure distribution (*NoPint*), the VAST solution became almost indistinguishable from the LS-DYNA solution.

Based on the investigation presented in this report, it is recommended to remove the atmospheric pressure from all finite element analyses to be performed within ComPropApp.

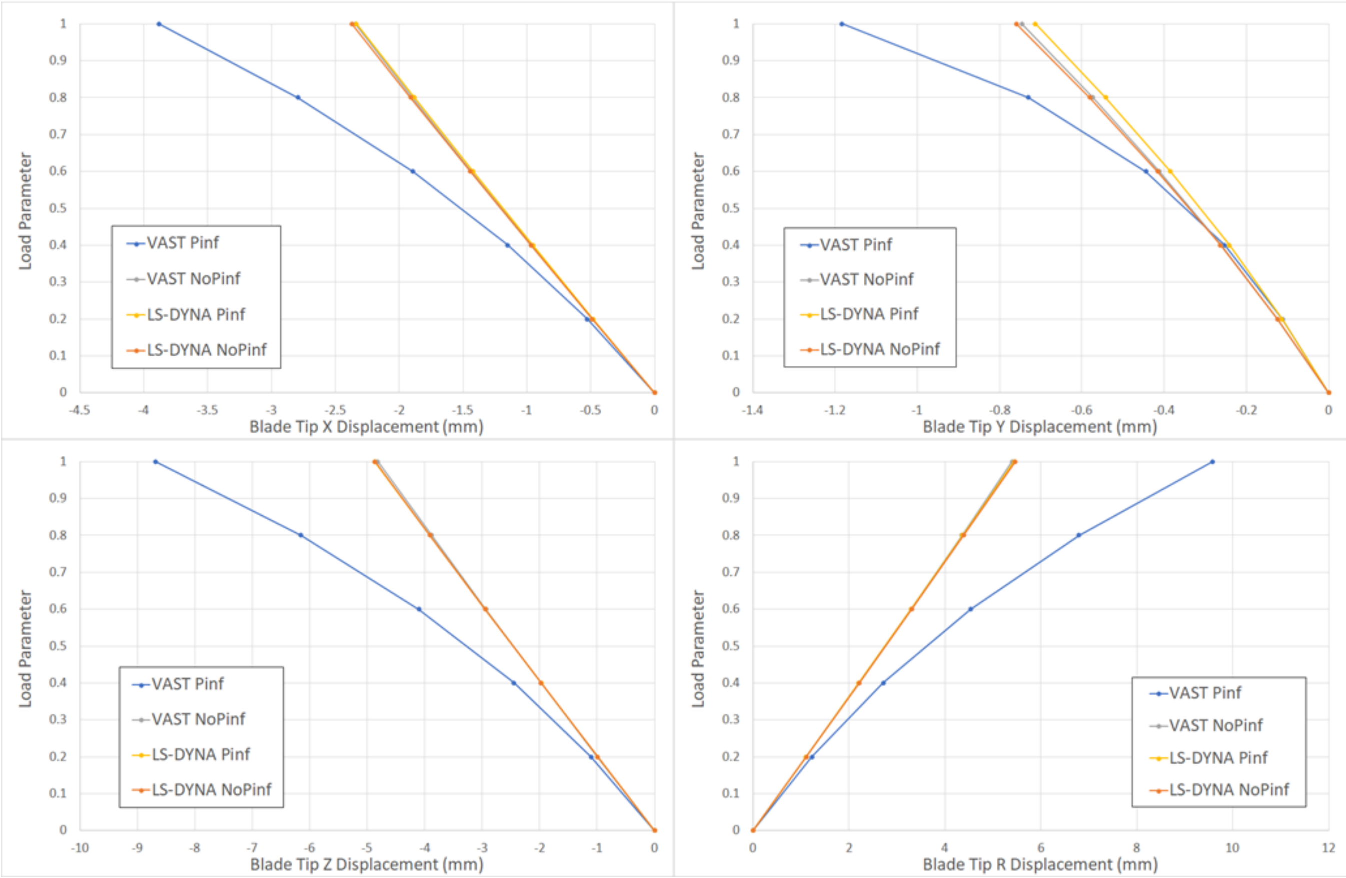

Figure 3-11: Comparison of VAST and LS-DYNA predicted load-deflection curves for solid element propeller models with and without the atmospheric pressure.

4. Incorporation of Failure Check Capability for Composite Materials

4.1 Tsai-Wu Failure Criterion

Tsai-Wu failure criterion [6] is one of the most used failure criteria today for assessing strength and failure of anisotropic and composite materials. In its general form, this failure criterion can be expressed as

$$F_1\sigma_1 + F_2\sigma_2 + F_3\sigma_3 + F_4\sigma_4 + F_5\sigma_5 + F_6\sigma_6 +$$

$$F_{11}{\sigma_1}^2 + F_{22}{\sigma_2}^2 + F_{33}{\sigma_3}^2 + F_{44}{\sigma_4}^2 + F_{55}{\sigma_5}^2 + F_{66}{\sigma_6}^2 +$$

$$2F_{12}\sigma_1\sigma_2 + 2F_{23}\sigma_2\sigma_3 + 2F_{31}\sigma_3\sigma_1 = 1$$

The coefficients and stress components in the above equation are defined from the material properties as

$$F_1 = \frac{1}{SXT} - \frac{1}{SXC};\; F_2 = \frac{1}{SYT} - \frac{1}{SYC};\; F_3 = \frac{1}{SZT} - \frac{1}{SZC};$$

$$F_4 = F_5 = F_6 = 0$$

$$F_{11} = \frac{1}{SXT \times SXC};\; F_{22} = \frac{1}{SYT \times SYC};\; F_{33} = \frac{1}{SZT \times SZC};$$

$$F_{44} = \frac{1}{SXY \times SXY};\; F_{55} = \frac{1}{SYZ \times SYZ};\; F_{66} = \frac{1}{SZX \times SZX};$$

$$F_{12} = f_{12}\sqrt{F_{11}F_{22}};\; F_{23} = f_{23}\sqrt{F_{22}F_{33}};\; F_{31} = f_{31}\sqrt{F_{33}F_{11}};$$

$$\{\sigma_1, \sigma_2, \sigma_3, \sigma_4, \sigma_5, \sigma_6\} = \{\sigma_X, \sigma_Y, \sigma_Z, \tau_{XY}, \tau_{YZ}, \tau_{ZX}\}$$

where SXT and SXC indicate the maximum tensile and compression stresses in the 1st material direction. SYT and SYC indicate the maximum tensile and compression stresses in the 2nd material direction. SZT and SZC indicates the maximum tensile and compression stresses in the 3rd material direction. SXY, SYZ, and SZX denote the maximum shear stresses in planes of symmetry. f12, f23, and f31 are the absolute interaction terms evaluated through material testing under biaxial stress state. For composite materials, the lamina material properties must be provided in the composite material property file Prefix. COM [2] and utilized in the evaluation.

For application to the shell elements, the above general form of the Tsai-Wu criterion reduces to

$$F_1\sigma_1 + F_2\sigma_2 + F_4\sigma_4 + F_{11}{\sigma_1}^2 + F_{22}{\sigma_2}^2 + F_{44}{\sigma_4}^2 + 2F_{12}\sigma_1\sigma_2 = 1$$

where the plane stress assumption is adopted so only the corresponding material properties, SXT, SXC, SYT, SYC, SXY and f12, are required in the input data file [2].

4.2 Implementation for Nonlinear Analysis

In the VAST implementation of the Tsai-Wu failure criterion, a safety factor, R, is computed at each evaluation point as

$$R(F_1\sigma_1 + F_2\sigma_2 + F_3\sigma_3 + F_4\sigma_4 + F_5\sigma_5 + F_6\sigma_6) +$$
$$R^2\,(F_{11}{\sigma_1}^2 + F_{22}{\sigma_2}^2 + F_{33}{\sigma_3}^2 + F_{44}{\sigma_4}^2 + F_{55}{\sigma_5}^2 + F_{66}{\sigma_6}^2) +$$
$$R^2\,(2F_{12}\sigma_1\sigma_2 + 2F_{23}\sigma_2\sigma_3 + 2F_{31}\sigma_3\sigma_1) = 1$$

The physical meaning of the safety factor is to scale the stresses at the evaluation point proportionally to reach the failure surface. As a result, safety factors less than one indicate failure.

This Tsai-Wu failure check was originally implemented in VAST for the linear dynamic analysis, but recently extended to nonlinear static analyses. These analysis types are referred to as the "unsteady" and "steady" analyses, respectively, in the ComPropApp environment. When the Tsai-Wu failure check is turned on in these analyses by setting NFAIL=2 in the Prefix.USE file, a Tecplot file, Prefix.TSF, is generated to provide the lowest safety factors in the material layer on the suction face (MINSF_SUC), the pressure face (MINSF_PRS) and through the entire thickness (MINSF_ALL) in each element at every time (for unsteady analysis) or load (for steady analysis) steps. This Tecplot data file can be readily utilized to generate contour plots of safety factors on various surfaces as shown in Figure 4-1 from which the potential failure can be identified.

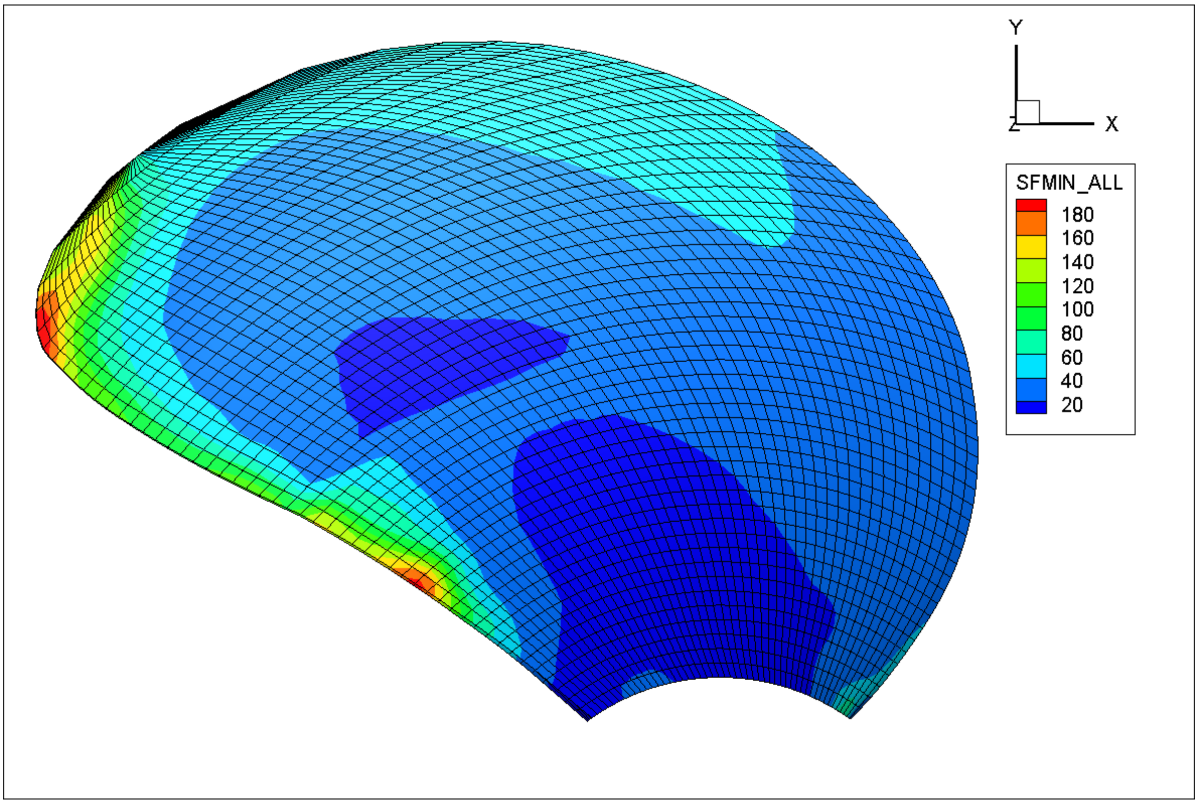

Figure 4-1: Minimum safety factor of all layers through the thickness of the ORCA model at the final load step.

5. Conclusions

This report described a recent refinement and further development of the VAST finite element solver for use in the Trident/PVAST system and the associated MARIN and CRS software tools for improved analysis and design of composite propellers. Three objectives were accomplished in this work:

First, the quadratic shell element in VAST was further enhanced to make it suitable for incorporation into the ComPropApp system. These enhancements included extension of the load modelling capability for consistency with the 20-noded solid element previous incorporated in ComPropApp. Also implemented in the shell element was the capability for outputting the results in the Tecplot format. These Tecplot files were generated based on the 16-noded option of the shell element so the complex geometry of the propellers can be accurately modelled and displayed. This shell element had been extensively tested for composite propeller analyses through collaboration with MARIN.

Second, the previously observed stress-softening behaviour in VAST nonlinear steady-state solutions for propellers was extensively investigated. After checking the nonlinear finite element formulation and its implementation in VAST, various details of the finite element propeller models were examined. This examination led to the discovery that the atmospheric pressure was included in the external load distribution. Inspired by this finding, a simple test case involving a cantilever beam was created and analysed using both VAST and LS-DYNA. This numerical exercise confirmed that the unrealistic stress-softening characteristics shown in the VAST solution was caused by the application of the atmospheric pressure that resulted in compression in the thickness direction. It has been indicated that if the atmospheric pressure is eliminated from the external load, VAST and LS-DYNA produced identical nonlinear solutions. For this reason, the temporary piecewise linear algorithm implemented in the earlier VAST was no longer required, so removed in the current version of the VAST solver.

Third, the Tsai-Wu failure criterion was successfully extended to nonlinear static analysis of composite structures and tested using the ORCA composite propeller model.

6. References

[1] Composite Propeller Design for Noise Reduction, A Proposal from Lloyds' Register Applied Technology Group, June 30, 2021

[2] VAST User's Manual, Version 9.2, Lloyds' Register Applied Technology Group, 2022

[3] Lampe, A., TECPLOT files for composite propeller, Private email communication, May 12, 2022.

[4] LS-DYNA Keywords User's Manual, Livermore Software Technology Corporation (LSTC), Livermore, California, 2017.

[5] Bathe, K.J., Finite Element Procedures, Prentice Hall, New Jersey, 1982.

[6] Tsai, S. W. and Wu, E. M. A General Theory of Strength for Anisotropic Materials. Journal of Composite Materials. 1971, Vol. 5, pp. 58-80.

Contact person
Lei Jiang
Software Development
237 Brownlow Ave, Suite 200
Dartmouth, NS B3B 2C7
Canada

Registered name Martec Limited

t: 1 (902) 417 2482
e: Lei.Jiang@lr.org
w: lr.org